



On the model granularity and temporal resolution of residential PV-battery system simulation



Benjamin Hauck^a, Weimin Wang^{b,*}, Yibing Xue^{c,**}

^a Department of Electrical Engineering and Information Technology, Karlsruhe Institute of Technology, Karlsruhe, Germany

^b Department of Engineering Technology, University of North Carolina at Charlotte, Charlotte, NC, USA

^c School of Architecture and Urban Planning, Shandong Jianzhu University, Jinan, China

ARTICLE INFO

Keywords:

Photovoltaic (PV)
Battery storage
Residential buildings
Self-sufficiency
Self-consumption

ABSTRACT

This paper investigates the impact of model granularity and temporal resolution on simulated energy flow items, self-sufficiency and self-consumption of grid-connected residential PV-battery systems. For such a purpose, three models with increasing levels of granularity are implemented for both PV modules and batteries. In addition, three temporal resolutions (i.e., 1 s, 1 min, and 1 h) of weather data and building electrical loads are considered. The simulation results for a PV-battery system in Lindenberg, Germany show that temporal resolutions have negligible impact on self-consumption and self-sufficiency, but cause noticeable differences of most power profiles observed in the PV-battery system. As for the impact of model granularity, the self-consumption is approximately 44% for the coarsest models, 48% for the models with the intermediate level of granularity, and 52% for the most refined models; the self-sufficiency is 83%, 78%, and 80%, respectively, for the three models.

1. Introduction

With the decreasing cost of photovoltaic (PV) modules and the rising concerns on environmental problems caused by fossil fuel consumption, solar PV has been the fastest growing distributed power generation technology. According to the U.S. Department of Energy (Feldman and Margolis 2020), there were 68 GW AC power capacity from PV in the U.S. by the end of September 2020. Of the 68 GW, 41 GW were utility-scale PV and 27 GW were distributed PV. Since 2010, the residential PV market has grown by approximately 40% per year on average, which has led to 14 GW AC power installed for residential PV systems in the U.S. More developed PV markets exist in some European countries. In Germany, for example, there was a total of about 43 GW of installed solar PV power by the end of 2017 (Wirth 2018), 74% of which were distributed on buildings, mostly on the rooftop of residential buildings. There are two basic types of residential PV systems: standalone (also known as off-grid PV systems) and grid-connected (also known as grid-tied or utility-interactive PV systems). The majority of residential PV systems are grid-connected, relying on the power grid at all times to balance the PV power supply and the building electricity demand. The ever-increasing penetration of solar PV into residential buildings contributes to a sustainable society by cutting user's utility bills, reducing fossil fuel

consumption and mitigating the greenhouse gas emissions to the environment. However, due to the intermittent nature of solar energy and the mismatch between power generation and power demand, a high penetration of PV capacity in the grid may lead to technical challenges of reliable power grid operation. Onsite storage devices, such as batteries, can be one of the effective means to not only smooth the PV system power generation and significantly increase the degree of autonomy, but also increase the economic return on investment.

There exist many studies on residential PV-battery systems, as demonstrated by the rich body of available publications included in a number of review papers (Chauhan and Saini 2014; Hoppmann et al., 2014; Luna-Rubio et al., 2012). From the perspective of PV-battery system design, numerous previous studies are related to either techno-economic analysis or optimal sizing. The work on techno-economic analysis (Brusco et al., 2016; Hoppmann et al., 2014; Kosmadakis et al., 2019; Linssen et al., 2017; Parra and Patel 2016; Silva and Hendrick 2017) intends to evaluate the costs, benefits, sensitivity factors, and uncertainties that could potentially affect the performance of PV-battery systems. Several performance metrics—such as self-consumption, self-sufficiency, levelized cost of energy, and life-cycle cost—are often used to facilitate the comparison of different system configurations and designs. The work on optimal sizing intends to apply optimization techniques for PV-battery system sizing. In this regard,

* Corresponding author.

** Corresponding author.

E-mail address: weimin.wang@uncc.edu (W. Wang).

<https://doi.org/10.1016/j.dibe.2021.100046>

Received 30 December 2020; Received in revised form 3 February 2021; Accepted 7 March 2021

Available online 11 March 2021

2666-1659/© 2021 The Authors. Published by Elsevier Ltd. This is an open access article under the CC BY-NC-ND license (<http://creativecommons.org/licenses/by-nc-nd/4.0/>).

Nomenclature	
A_{PV}	PV module area (m^2)
Cap_{Wh}	energy capacity of the battery (Wh)
E_{g0}	bandgap of PV material (eV)
G_{total}	total solar irradiance on PV modules (W/m^2)
k_B	Boltzmann constant (J/K)
K_i	temperature dependence of the short circuit current (A/K)
I	electric current (A)
I_0	reverse saturation current (A)
$I_{0,STC}$	reverse saturation current at the standard test conditions (A)
I_{ph}	PV photocurrent (A)
I_{SC}	short circuit current of a PV module at the standard test conditions (A)
MPP	maximum power point
n	ideality factor
$n_{cycle,t}$	number of battery charging/discharging cycles at time t
N_s	number of cells in series of a PV module
$NOCT$	nominal operating cell temperature (K)
P	real power (W)
$P_{bat,DC}$	DC power charged into (+) or discharged from (-) the battery (W)
P_{charge}	power used to charge the battery (W)
$P_{discharge}$	power discharged from the battery (W)
$P_{grid,export}$	power exported to the grid (W)
$P_{grid,import}$	power imported from the grid (W)
P_{load}	building electrical load (W)
P_{PV}	AC power generated by the PV modules (W)
$P_{PV,DC}$	DC power generated by the PV modules (W)
q	electron charge (Coulomb)
Q	useable capacity of the battery at a given current (Ah)
R_s	series resistance of a PV cell (Ω)
R_{sh}	shunt resistance of a PV cell (Ω)
SC	self-consumption
SOC	battery state of charge
SOC_{min}	minimum limit of battery state of charge
SOC_{max}	maximum limit of battery state of charge
SS	self-sufficiency
t	time (hour)
T_{air}	ambient air temperature (K)
T_{cell}	operating temperature of solar cells (K)
V	voltage (V)
V_{bat}	battery voltage (V)
V_{cutoff}	battery cut-off voltage when discharging (V)
V_{max}	battery maximum allowed voltage when charging (V)
V_{OC}	open circuit voltage of a battery cell (V)
α_{cycle}	battery cyclic aging factor
$\alpha_{calendar}$	battery calendric aging factor
β	temperature coefficient of PV electrical efficiency (1/K)
$\eta_{charger}$	battery inverter/charger efficiency
$\eta_{PV, rated}$	PV module rated electrical efficiency
$\eta_{PV, temp}$	PV module electrical efficiency at an operating temperature

Mulder et al. (2013) determined the optimal sizing of a PV-battery systems in the context of different remuneration schemes (i.e., the combination of different selling prices and self-consumption fees of PV power). Okoye and Solyali (2017) developed a mixed integer linear programming (MILP) model to optimize the size of standalone residential PV-battery systems. Li (2019) applied a genetic algorithm to size residential PV-battery systems for minimizing the total annual cost of electricity. Mulleriyawage and Shen (2020) used MILP to optimally size the battery storage capacity for minimizing annual cost including both energy and battery degradation-based cost. Ru et al. (2013) developed an optimization model to determine the battery size for grid-connected PV systems for the purpose of power arbitrage and peak shaving. Zhang et al. (2017) applied a multi-objective genetic algorithm to optimize the battery size and operation parameters, towards maximizing the self-sufficiency and net present value of a PV-battery system.

All aforementioned studies on techno-economic analysis and optimal sizing rely on electrical load profiles and PV generation profiles as the key inputs. In these studies, building electrical load profiles are usually assumed to be known in advance, which can be obtained by either field measurements or simulation models. For PV power profiles, some studies (e.g., Beck et al., 2016; Langenmayr et al., 2020; Linssen et al., 2017) rely on field measurements to establish these profiles while others (e.g., Hoppmann et al., 2014; Zhang et al., 2017) calculate PV power from meteorological data (e.g., solar irradiance and air temperature). Whenever the data are sourced from, the temporal resolutions of PV power and building electrical load profiles need to be considered carefully because they may affect system performance evaluation. Most previous studies have used the temporal resolution ranging from 1 min to 1 h.

In addition to temporal resolution, the granularity of PV-battery system models has impact on the accuracy of results as well. In this paper, the granularity refers to the level of detail captured when abstracting the reality of PV and battery behaviour in the modelling process. By considering more state variables, parameters, and lower-level processes, a model with fine granularity leads to higher fidelity of results

than a model with coarse granularity. However, a finer-grained model takes more effort to develop and validate, and may result in an increased computational cost. A variety of models for PV modules and batteries are observed in previous studies. For PV models, Ru et al. (2013) calculated the PV power simply from the rated efficiency and solar irradiance. Okoye and Solyali (2017) considered the impact of PV cell temperature and aging on power generation. Ibrahim et al. (2017) used a random forest model to predict PV power generation, which requires a large set of measured data, such as PV power, solar radiation, and ambient temperature be available to train the random forest model. Zhang et al. (2017) used an electrical equivalent single-diode model to capture the current-voltage characteristics of PV modules. For battery modelling, except for Zhang et al. (2017), who used an improved Shepherd battery model, the majority of previous studies used simple battery models. These simple battery models do not capture battery voltage and current characteristics and thus cannot consider the dynamic behaviour of battery charging and discharging processes.

Both temporal resolution and model granularity are regarded important considerations in PV-battery system performance assessment (Ibrahim et al., 2017) because they affect the accuracy of simulation results, the efforts of model development and implementation, the computation time (especially for design optimization), and even data availability. Therefore, understanding the impact of temporal resolution and model granularity on PV-battery system performance is important for techno-economic analysis and optimal design of PV-battery systems. However, there exists limited work in this niche area except for a few studies on the impact of temporal resolutions. For example, Beck et al. (2016) calculated the self-consumption of a PV-battery system with different temporal resolutions (namely, 10s, 30s, 1 min, 5 min, 15 min, and 1 h) of PV power and building electrical load. They found that temporal resolutions had negligible impact on the result of self-consumption. Ried et al. (2015) made a similar conclusion that different temporal resolutions (i.e., 1 min, 5 min, 15 min, and 1 h) had minor impact on self-consumption and self-sufficiency of residential PV

battery systems. However, they found that the number of battery full cycles was underestimated by 11% with the use of 1-h temporal resolution relative to the 1-min temporal resolution. [Burgio et al. \(2020\)](#) studied the impact of temporal resolution and time averaging on the performance analysis of a PV-battery system. Three temporal resolutions (i.e., 15, 30, and 60 min) were obtained from the 3-min load profile of a real building. They concluded that the temporal resolution had negligible impact on the calculation of savings on the electricity bills but the 60-min load profile substantially underestimated both the feed-in and the withdrawal contractual power by 21% and 38%, respectively.

This paper intends to investigate the impact of model granularity and temporal resolution on performance simulation of residential PV-battery systems. The major contributions of this paper include the following. First, the paper fills a knowledge gap in literature that lacks the study on how the granularity of modelling PV modules and batteries affects system performance simulation. Second, the paper corroborates a few earlier studies on the impact of temporal resolutions of building electrical load and PV power on certain performance metrics. Third, the findings on how power flows, self-consumption and self-sufficiency change with model granularity and temporal resolutions are important to support future research by shedding light on the proper selection of component models and input data resolutions for the performance simulation of PV-battery systems. In the rest of this paper, the analytical approach is presented first. Then, the PV models and the battery models are sequentially described in Sections 3 and 4. Simulation inputs, such as building load, weather data, and PV and battery parameters, are provided in Section 5. Results are presented and discussed in Section 6. The paper ends with some conclusions and suggestions for future work.

2. Approach

2.1. PV-battery system configuration and controls

In general, depending on the point of battery connection, residential PV-battery systems can be configured as direct current (DC) coupled systems and alternating current (AC) coupled systems. DC-coupled systems have the battery connected to the DC link of the PV inverter while AC-coupled systems have the battery connected to the PV output via a bidirectional battery inverter. AC-coupled systems are prevalent because they are easily reconfigurable and generally more efficient in applications where PV energy is mostly used at the time of generation ([Ardani et al., 2016](#)). Therefore, this paper considers an AC-coupled PV-battery system that consists of PV modules, a PV inverter, a battery stack, a battery inverter charger, electrical accessories (e.g., wires, overcurrent protection devices, junction boxes, and switches) and structural components (e.g., PV mounting systems). The photovoltaic modules are mounted on the building roof and are connected to a single-phase inverter. A bidirectional inverter connects the battery to the AC side of the system. All electrical loads inside the household are connected to the system on the AC side. The system itself is grid connected. [Fig. 1](#) shows

possible power flows between the system components.

This study uses a simple control mechanism ([Fig. 2](#)) commonly deployed in existing PV-battery systems. The core idea underlying the simple control mechanism includes: 1) building electrical demand is satisfied first by the PV power, then by the battery and finally by the grid and 2) excess PV power is first stored in the battery and the remaining power is then exported to the grid. When the battery is charged or discharged, a couple of constraints need to be followed. First, the battery's state of charge (SOC) must be within its boundary values (i.e., SOC_{min} and SOC_{max}) at all times. Second, the AC power charged to (P_{charge}) or discharged from ($P_{discharge}$) the battery must be within certain limits, which are determined differently depending on how the battery is modelled. For example, the battery charging power limit may be set to ensure the SOC after charging to be less than SOC_{max} , or it can be set to ensure the battery voltage limit is not exceeded.

2.2. Performance metrics

The performance of residential PV-battery systems can be evaluated with different metrics, representatives of which include self-consumption, self-sufficiency, and economic performance criteria such as levelized cost of energy, net present value, and life-cycle cost. All these performance metrics are derived from the series of power flows over a certain study period. Therefore, we will investigate the impact of model granularity and temporal resolution on power flow items, self-consumption and self-sufficiency. Economic performance metrics are not covered in this paper because all economic parameters (e.g., the discount rate and the interest rate), capital costs, and electricity tariff are highly location-dependent and thus make it difficult to make generic conclusions.

Self-consumption (SC) is defined as the electricity generated by PV that is consumed locally by the household divided by the overall PV generation. Using the power flow items in [Fig. 1](#), the equation to calculate SC is expressed as:

$$SC = \frac{\sum P_{PV} - \sum P_{grid,export}}{\sum P_{PV}} \quad (1)$$

where all summations are made across the system operating life.

Self-sufficiency (SS) describes the share of the household electricity consumption that is supplied by the PV-battery system. SS is calculated as:

$$SS = \frac{\sum P_{load} - \sum P_{grid,import}}{\sum P_{load}} \quad (2)$$

3. PV simulation models

Three PV simulation models are considered in this paper with increasing levels of granularity. All three models calculate the PV power

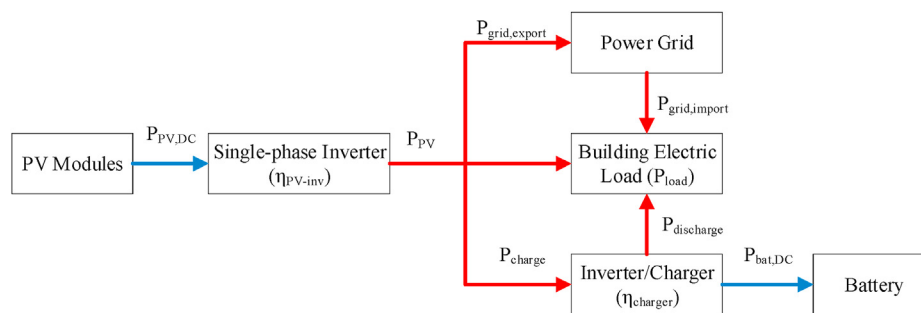


Fig. 1. Visualization of possible power flows between PV electricity generation, battery storage, power grid and electrical loads. Red lines indicate the AC power while blue lines indicate the DC power. Power flows along the line directions are positive. (For interpretation of the references to colour in this figure legend, the reader is referred to the Web version of this article.)

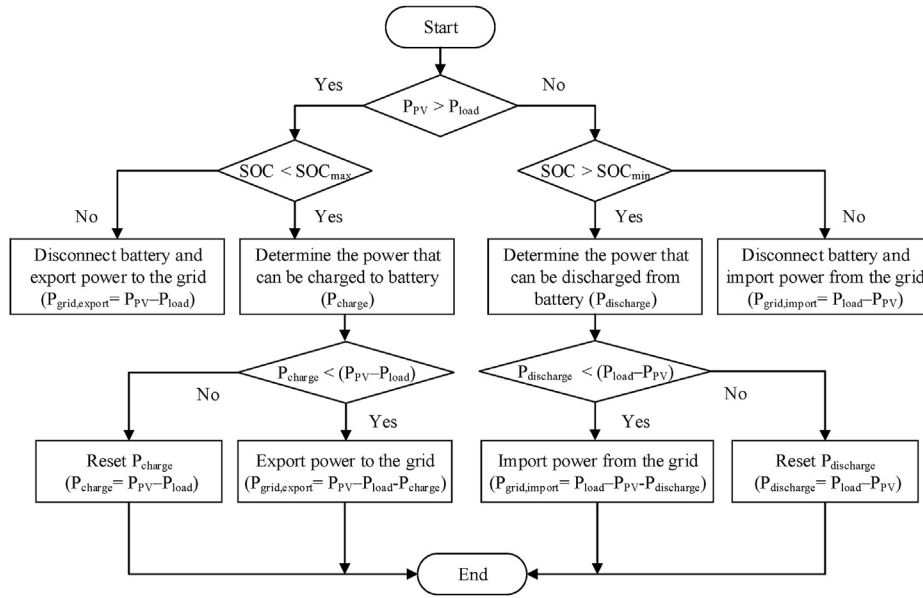


Fig. 2. Flowchart of the control mechanism used for the PV-battery system.

based on weather variables, including solar irradiance and ambient temperature.

3.1. PV model 1

As the simplest one of the three models considered, Model 1 assumes that the PV modules operate at their rated efficiency throughout its entire life.

3.2. PV model 2

PV Model 2 uses a similar approach as Model 1, but captures the impact of cell temperature and aging on PV electrical efficiency. To account for the temperature impact, the following equation is used (Dubey et al., 2013):

$$\eta_{PV,temp} = \eta_{PV, rated} \left[1 - \beta \left(T_{air} + \frac{NOCT - 293}{800} G_{total} - 298 \right) \right] \quad (3)$$

where, $\eta_{PV, rated}$ and $\eta_{PV,temp}$ represents the PV module efficiency respectively at standard testing conditions (STCs) and at an operating temperature different from the STCs; β is the temperature coefficient (1/K) that varies with PV materials; NOCT is the nominal operating cell temperature (K) and T_{air} the ambient air temperature (K); G_{total} is the total solar irradiance on PV modules (W/m^2).

The degradation of PV modules under actual operating conditions is due to environmental stresses, such as temperature, moisture, thermal cycling, ultraviolet light exposure, and high voltage (Sharma and Chandel 2013). PV degradation due to aging is modelled as a constant degradation rate per year, which is evenly distributed to all time steps used in the simulation.

3.3. PV model 3

Simulation model 3 is based on an equivalent electrical circuit for PV cells, as shown in Fig. 3. The circuit consists of a current source, a diode, a shunt resistance (R_{sh}) and a series resistance (R_s) (Nguyen and Nguyen 2015). The model includes the electrical behaviour of solar cells and is therefore more realistic than the efficiency-based models.

For most PV modules, solar cells are connected in series to obtain an adequate working voltage. Let N_s denote the number of cells serially connected in a PV module, the following equations are used by PV Model

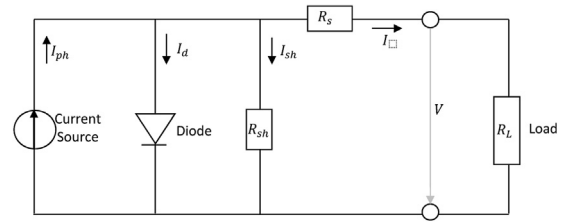


Fig. 3. PV cell electrical equivalent circuit.

3 (Nguyen and Nguyen 2015).

The solar irradiance G_{total} leads to the cell photocurrent I_{ph} :

$$I_{ph} = [I_{SC} + K_i(T_{cell} - 298)] \cdot \frac{G_{total}}{1000} \quad (4)$$

where, I_{SC} is the short circuit current in Ampere (A) at the STCs; K_i , in A/K, is the temperature dependence of the short circuit current.

At the STCs, the cell's reverse saturation current $I_{0,STC}$ is obtained by:

$$I_{0,STC} = \frac{I_{SC}}{\exp\left(\frac{q \cdot V_{OC}}{N_s \cdot k_B \cdot n \cdot T_{cell}}\right) - 1} \quad (5)$$

where, $q = 1.602 \cdot 10^{-19}$ is the electron charge in Coulomb; V_{OC} is the open circuit voltage (V) of a PV module at the STCs; $k_B = 1.381 \cdot 10^{-23}$ J/K is the Boltzmann constant; and n is the ideality factor of the diode.

The reverse saturation current varies with cell temperature, which is described as:

$$I_0 = I_{0,STC} \left[\frac{T_{cell}}{298} \right]^3 \exp \left[\frac{q E_{g0}}{n k_B} \left(\frac{1}{298} - \frac{1}{T_{cell}} \right) \right] \quad (6)$$

where, E_{g0} is the semiconductor's bandgap (1.1 eV for silicon).

For a PV module, the voltage-current characteristic equation is given as:

$$I(V) = I_{ph} - I_0 \left[\exp \left(\frac{q \left(\frac{V}{N_s} + I R_s \right)}{n k_B T} \right) - 1 \right] - \frac{V}{R_{sh}} + I R_s \quad (7)$$

where, R_S is the series resistance (Ohm, Ω) of a solar cell; and R_{sh} is the shunt resistance (Ω) of a solar cell.

Based on Eq. (7), the maximum power point (MPP) can be found. This MPP multiplied by the number of installed modules is then regarded as the PV array's electric power output ($P_{PV,DC}$). Once the DC power output is available, the AC power (P_{PV} , see Fig. 1) can be calculated after accounting for the PV inverter efficiency and the power factor.

4. Battery simulation models

In parallel with PV models, this paper considers three battery models with increasing levels of granularity. The first two models simplify battery as an "energy bucket" that holds a quantity of electrical energy. Energy can be released from or stored into the bucket as long as the amount of energy in the bucket satisfies its limits. In contrast to the first two models, the third model is more sophisticated by capturing the battery's electrochemistry behaviour to some extent. It needs to be noted that several different types of battery (e.g., lead acid and lithium-ion) can be deployed in residential PV systems. Because lithium-ion batteries are increasingly used for residential electrical storage, they are the primary consideration in the battery models discussed here.

4.1. Battery model 1

Battery Model 1 simulates an ideal storage device without performance degradation. At any given time, the amount of energy that can be charged to or discharged from the battery is merely subject to the constraint of the battery's minimum and maximum SOC requirement. In this model, the battery's SOC is continuously tracked according to:

$$SOC_{t+\Delta t} = SOC_t + \frac{P_{bat,DC}(t)\Delta t}{Cap_{wh}} * 100 \quad (8)$$

$$P_{bat,DC} = \begin{cases} P_{charge} * \eta_{charger} & (charging) \\ \frac{P_{discharge}}{\eta_{charger}} & (discharging) \end{cases} \quad (9)$$

where, $P_{bat,DC}$ is the DC power (W); P_{charge} and $P_{discharge}$ represents the AC power (W) respectively for charging and discharging (see Fig. 1); Cap_{wh} is the battery's initial energy capacity (Wh); $\eta_{charger}$ is the energy efficiency of the battery charger.

4.2. Battery model 2

In comparison with battery Model 1, Model 2 accounts for the battery's roundtrip efficiency and the impact of aging on battery performance. Modelling battery aging and life expectancy is an active research subject. In general, the lifetime of lithium-ion batteries strongly depends on the ambient temperature and the charge/discharge rates. One direct outcome of aging is the increase of internal battery resistance, which degrades cell performance (e.g., reduced energy capacity) over the battery's lifetime. Model 2 considers two aging mechanisms: cycle aging and calendar aging. Cycle aging refers to the degradation of electrode active materials' reversibility, caused by the use of battery. Calendar aging comprises all aging processes that degrade battery cells independent of charging and discharging cycles. The predominant mechanism of calendar aging is the evolution of passivation layers caused by interactions between electrolyte and electrode active materials (Keil et al., 2016).

Due to the consideration of battery aging, Model 2 has an ever-decreasing energy capacity expressed as:

$$Cap_{wh,t} = Cap_{wh} \left(1 - \alpha_{cycle} n_{cycle,t} - \alpha_{calendar} \frac{t}{8760} \right) \quad (10)$$

where, $n_{cycle,t}$ is the number of battery charging/discharging cycles; α_{cycle} and $\alpha_{calendar}$ are the cyclic and calendric aging factors.

In this model, in addition to the charger efficiency, the battery's roundtrip efficiency is considered and it is introduced into Eq. (9) in a similar manner as $\eta_{charger}$, attributing the storage losses equally to charging and discharging as the square root of the roundtrip efficiency.

4.3. Battery model 3

Battery Model 3 differs from the previous two simple battery models because it is based on an electrical equivalent circuit (Yao et al., 2013) for a battery cell. As Fig. 4 shows, the circuit consists of a voltage source, a series resistance R_0 and two resistor-capacitor (RC) elements (i.e., R_1C_1 and R_2C_2). The voltage source represents the open circuit voltage (V_{OC}), the value of which depends on the battery's SOC. The series resistance mainly captures the electrolyte resistance whereas the two RC-elements represent the contact resistance and the contact capacitance between the electrolyte and the anode and the cathode, respectively.

Electric current (I) is the main input variable for this battery model. Based on the electric current, the procedure of determining the battery voltage (V_{bat}) is described below:

Step 1. Determine the battery's SOC:

$$SOC_{t+\Delta t} = SOC_t + \frac{I(t)\Delta t}{Q} * 100 \quad (11)$$

where Q is battery's useable capacity in Ah for the given electric current.

Step 2. Calculate the battery's open circuit voltage (V_{OC}) based on the SOC from Step 1. The relationship between V_{OC} and SOC needs to be predefined.

Step 3. Calculate the battery's overvoltage. The overvoltage comes from the voltage over the series resistance R_0 and the voltage over the two RC-elements.

Step 4: Calculate the battery's voltage V_{bat} by adding the overvoltage to the open circuit voltage.

Step 5: Once the battery voltage is calculated, it is checked against the battery's operation limits. If the battery voltage falls below the cut-off voltage (V_{cutoff}) when discharging, or exceeds the maximum allowed voltage (V_{max}) when charging, the battery is disconnected to prolong its life expectancy.

Battery Model 3 considers aging and the roundtrip efficiency in the same manner as battery Model 2.

5. Building load, weather data and simulation parameters

5.1. Building electrical load

Electricity is used in buildings for different energy end uses such as space heating, cooling, lighting and plug loads. Precise electrical load profiles of households can be measured in the field or calculated from energy simulation software. Because the paper concentrates on PV-battery systems, building electrical load profile is directly taken from

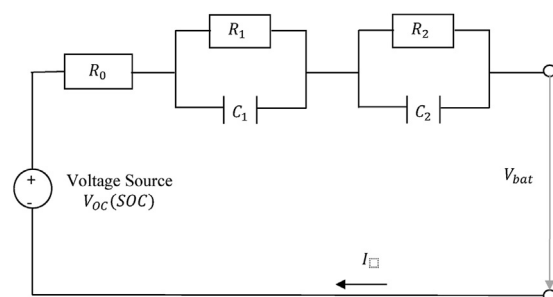


Fig. 4. Battery cell electrical equivalent circuit.

the literature. Tjaden et al. (2015) compiled a total of 74 freely accessible residential load profiles for single-family households. All load profiles are synthesized from field measurements and have 1-s intervals. The first load profile is used in this paper. Each data point in the load profile comprises of three phases of active and reactive power. The power values of the three phases are summed up to obtain the active power and reactive power, based on which the power factor can be derived.

The load profile has an annual electricity consumption of 3240 kWh and a peak load of 22 kW occurred in the early morning on January 28. The annual daily average load demand is 8.9 kWh/day. Fig. 5 shows the daily profile averaged across the whole year. However, it must be noted that actual daily profiles have much greater fluctuations, which will be further discussed in Section 6.

5.2. Weather data

The Baseline Surface Radiation Network (2018) provides weather data of 1-min intervals for many locations over the world. The weather data for Lindenberg, Germany (Latitude 52.2°, Longitude 14.1°) in the year of 2012 are used in this paper. Specifically, weather data used to support this work includes the global horizontal solar irradiance, the diffuse horizontal solar irradiance, the direct normal solar irradiance, and the air temperature. These data are pre-processed to deal with missing or evidently unreasonable values (e.g., air temperature more than 40 °C and solar irradiance being negative). After cleaning, the global horizontal solar irradiance has a peak value of 1072 W/m² and a minimum value of 0. The weather data indicates an annual global horizontal solar irradiance of 1120 kWh. Fig. 6 shows the daily solar irradiance profiles averaged across the whole year. Again, actual solar irradiance profiles have much greater fluctuations than what Fig. 6 shows.

Because PV modules are usually tilted on the roof, solar irradiance values in the weather data need to be processed further to obtain the total solar irradiance G_{total} on the PV surface, as used in Eqs. (3) and (4). Based on the isotropic sky diffuse model, the total solar irradiance consists of three components: beam, isotropic diffuse, and solar radiation diffusely reflected from the ground, for which the calculation can be found in Duffie and Beckman (2013).

5.3. PV-battery system specifications

Commercial PV modules (SW 250 mono) from SolarWorld (2018) are referred to set the PV parameters (Table 1), where most parameter values are taken from the manufacturer's product data sheets.

Table 2 provides the lithium-ion battery cell parameters, the values of

most which are for the lithium ferro phosphate battery as discussed in Yao et al. (2013). Fig. 7 shows the modelled open circuit voltage curve relative to the cell's state of charge (SOC). For a single cell, the maximum charge voltage ($V_{max} = 3.55V$) corresponds to the SOC of 100% while the discharge cut-off voltage ($V_{cutoff} = 2.65V$) corresponds to the SOC of 0. In this work, the open circuit voltage curve in Fig. 7 is implemented as a 16th order regression equation.

In addition to the PV and battery parameters, there are several other miscellaneous parameters. The PV inverter and the battery charger/inverter have a constant efficiency of 97% and 94%, respectively. The battery has a roundtrip efficiency of 88%.

6. Results and discussion

Implemented in MATLAB, the PV-battery system simulation model is generic to handle different inputs, including weather data, building electrical loads, and PV and battery parameters. Based on the typical roof area available for PV installation and system design in Germany, PV and batteries are sized in this paper as follows: the PV array, consisting of 2 strings of 12 serially connected modules, has a rated DC power of 6 kW; the battery stack, consisting of 14 cells in series and 300 cells in parallel, has a maximum energy capacity of 16.3 kWh.

6.1. Simulation matrix

The model granularity for PV and battery simulations, as discussed in Sections 4 and 5, increases from low (or coarse) corresponding to Model 1 to high (or refined) corresponding to Model 3. In addition to model granularity, three different temporal resolutions, namely, 1 s, 1 min, and 1 h, are considered for building load and weather data. The combination of model granularity and temporal resolution leads to the simulation matrix shown in Table 3. In this table, the model granularity refers to the case of having the same level of granularity for both PV and battery. For example, the low level of granularity has PV Model 1 and battery Model 1. The combinations of PV and battery models with mixed levels of granularity are not pursued. In addition, the scenario of running the refined models with hourly data is not pursued because the charging and discharging characteristics in the detailed battery model make sense only for short timesteps.

Recall that in Section 5, the original source of building electrical load has 1-s intervals while the original source of weather data has 1-min intervals. To perform simulations at temporal resolutions different from the time intervals of the original data source, we use the averaging operation on relevant variables (e.g., electrical load, solar irradiance, and

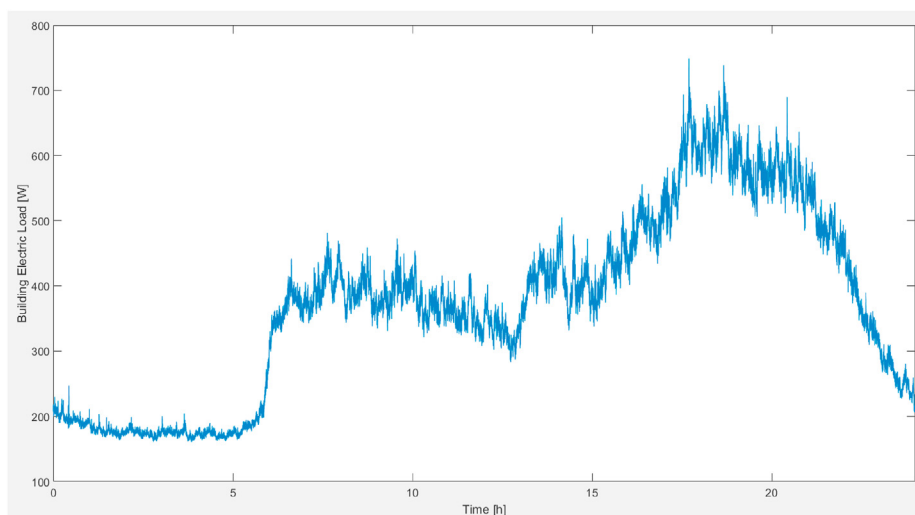


Fig. 5. Annual average daily electrical load profile.

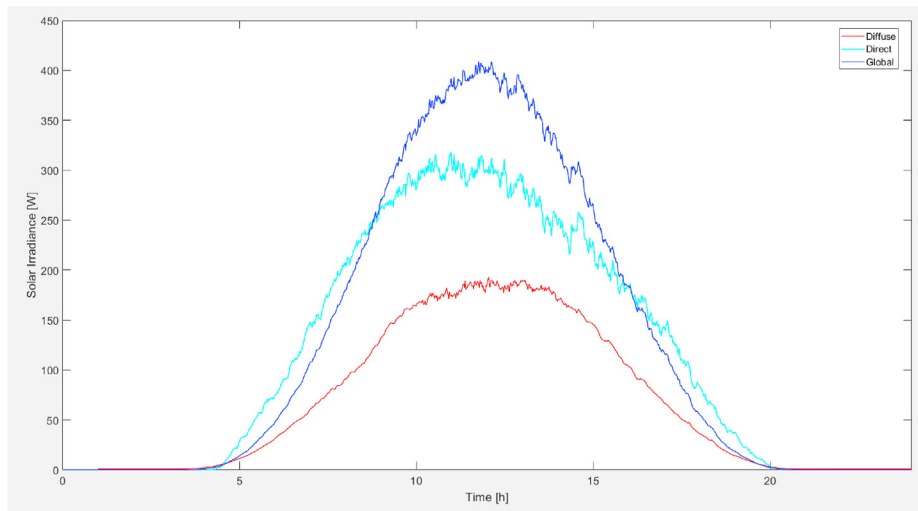


Fig. 6. Annual average daily solar irradiance profile.

Table 1
PV module parameters.

Parameter Name	Symbol	Value	Reference
Number of cells in series per module	N_s	60	SolarWorld (2018)
Ideality factor	n	1.2	Nguyen and Nguyen (2015)
Cell series resistance	R_s	0.0001 Ω	Nguyen and Nguyen (2015)
Cell shunt resistance	R_{sh}	1000 Ω	Nguyen and Nguyen (2015)
Temperature dependence of I_{sc}	K_i	0.00004 A/K	SolarWorld (2018)
Nominal operating cell temperature	NOCT	46°C	SolarWorld (2018)
Area per solar module	A_{module}	1.677 m^2	SolarWorld (2018)
Module open circuit voltage	V_{oc}	37.8 V	SolarWorld (2018)
Module short circuit current	I_{sc}	8.28 A	SolarWorld (2018)
Annual PV aging factor	$\eta_{PV,loss}$	0.5 %	Jordan and Kurtz (2013)
Rated efficiency	$\eta_{PV,rated}$	14.91 %	SolarWorld (2018)
Temperature coefficient	β	0.0045/K	SolarWorld (2018)

Table 2
Lithium-ion cell parameters.

Parameter Name	Symbol	Value	Reference
Capacity	Q_{cell}	1.1Ah	Yao et al. (2013)
Energy capacity	$Cap_{wh,cell}$	0.0039kWh	Yao et al. (2013)
Cycle aging	α_{cycle}	0.0022 %/cycle	Ansean et al. (2016)
Calendar aging	$\alpha_{calendar}$	2 %/year	Leadbetter and Swan (2012)
Cell series Resistance	R_0	0.08 Ω	Yao et al. (2013)
Resistance R_1	R_1	0.015 Ω	Yao et al. (2013)
Capacitor C_1	C_1	800 F	Yao et al. (2013)
Resistance R_2	R_2	0.05 Ω	Yao et al. (2013)
Capacitor C_2	C_2	4000 F	Yao et al. (2013)
Minimum SOC	SOC_{min}	10%	Parra and Patel (2016)
Maximum SOC	SOC_{max}	90%	Parra and Patel (2016)

ambient air temperature). For example, the hourly ambient air temperature is obtained by averaging the temperature of all 60 min within that hour. Similarly, the ambient air temperature in all 60 s is assumed the same as that at the corresponding minute.

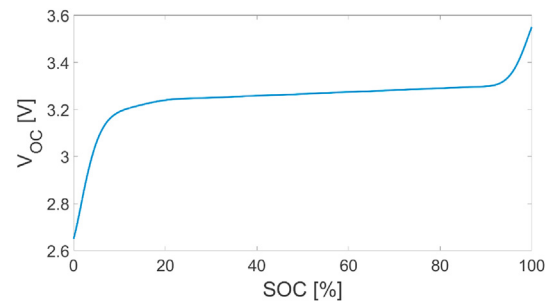


Fig. 7. Battery cell's open circuit voltage vs. state of charge.

Table 3
Simulation matrix resulted from different considerations of model granularity and temporal resolution.

Model Granularity Level	Temporal Resolution		
	1 s	1 min	1 h
Low (Model 1)	X	X	X
Intermediate (Mode 2)	X	X	X
High (Model 3)	X	X	-

6.2. Comparison of energy flows

The PV-battery system has been simulated for 20 years. Table 4 summarizes different energy flow items within three years (i.e., 1st, 10th, and 20th) for all 8 simulation scenarios. Fig. 1 can be referred to for the meanings of the energy flow items. In Table 4, for each temporal resolution, the numbers in parentheses under the columns of Mode 1 and Model 3 indicate the percentage differences of the results relative to the intermediate level of model granularity (Mode 2). Table 4 shows the following:

- Energy balance was maintained for all simulation runs, as demonstrated by the sum of energy supply (i.e., PV, battery discharge, and grid import) being equal to the sum of energy consumption (i.e., load, battery charge, and grid export).
- The coarse models (Model 1) had the same results across different years because they did not consider the impact of aging on PV and

Table 4

Annual energy flows of the modelled PV-battery system for the 1st, 10th, and 20th years. All energy flows have the unit of kWh.

Year	Energy Item	Temporal Resolution and Model Granularity							
		1 h		1 min			1 s		
		Model 1	Model 2	Model 1	Model 2	Model 3	Model 1	Model 2	Model 3
1st	PV ($\sum P_{PV}$)	6459 (3%)	6251	6589 (4%)	6323	5927 (-6%)	6591 (4%)	6324	5929 (-6%)
	Battery discharge ($\sum P_{discharge}$)	1351 (2%)	1331	1460 (2%)	1436	1395 (-3%)	1470 (2%)	1446	1402 (-3%)
	Grid import ($\sum P_{grid,import}$)	562 (-1%)	569	555 (-2%)	569	633 (11%)	556 (-2%)	569	637 (12%)
	Load ($\sum P_{load}$)	3239 (0%)	3239	3239 (0%)	3239	3239 (0%)	3239 (0%)	3239	3239 (0%)
	Battery charge ($\sum P_{charge}$)	1524 (-8%)	1663	1647 (-8%)	1794	1751 (-2%)	1659 (-8%)	1807	1762 (-2%)
10th	Grid export ($\sum P_{grid,export}$)	3609 (11%)	3250	3719 (13%)	3294	2965 (-10%)	3719 (13%)	3294	2967 (-10%)
	PV ($\sum P_{PV}$)	6459 (8%)	5969	6589 (9%)	6037	5660 (-6%)	6591 (9%)	6039	5661 (-6%)
	Battery discharge ($\sum P_{discharge}$)	1351 (7%)	1265	1460 (7%)	1364	1382 (1%)	1470 (7%)	1374	1389 (1%)
	Grid import ($\sum P_{grid,import}$)	562 (-13%)	645	555 (-15%)	652	657 (1%)	556 (-15%)	653	662 (1%)
	Load ($\sum P_{load}$)	3239 (0%)	3239	3239 (0%)	3239	3239 (0%)	3239 (0%)	3239	3239 (0%)
20th	Battery charge ($\sum P_{charge}$)	1524 (-4%)	1587	1647 (-4%)	1711	1741 (2%)	1659 (-4%)	1723	1753 (2%)
	Grid export ($\sum P_{grid,export}$)	3609 (18%)	3054	3719 (20%)	3104	2720 (-12%)	3719 (20%)	3104	2721 (-12%)
	PV ($\sum P_{PV}$)	6459 (14%)	5656	6589 (15%)	5720	5363 (-6%)	6591 (15%)	5722	5364 (-6%)
	Battery discharge ($\sum P_{discharge}$)	1351 (41%)	956	1460 (52%)	960	1372 (43%)	1470 (53%)	963	1379 (43%)
	Grid import ($\sum P_{grid,import}$)	562 (-42%)	967	555 (-48%)	1070	681 (-36%)	556 (-48%)	1077	685 (36%)
	Load ($\sum P_{load}$)	3239 (0%)	3239	3239 (0%)	3239	3239 (0%)	3239 (0%)	3239	3239 (0%)
	Battery charge ($\sum P_{charge}$)	1524 (27%)	1199	1647 (37%)	1203	1729 (44%)	1659 (37%)	1208	1741 (44%)
	Grid export ($\sum P_{grid,export}$)	3609 (15%)	3141	3719 (12%)	3308	2449 (-26%)	3719 (12%)	3316	2449 (-26%)

battery. In contrast, Model 2 and Model 3 had different results (except for the load) across different years because of their consideration of aging impact. Annual PV aging factor was modelled at 0.5%; hence, the PV energy generated at the 10th year and the 20th year reduced, respectively, by 5% and 10% relative to the 1st year.

For a given model granularity, the temporal resolution had a minor impact on the simulated energy flows. Relative to the simulation results with 1-min temporal resolution of input data, the corresponding energy flows with 1-s resolution of data had less than 1% difference whereas the energy flows with 1-h resolution of data had up to about 10% difference.

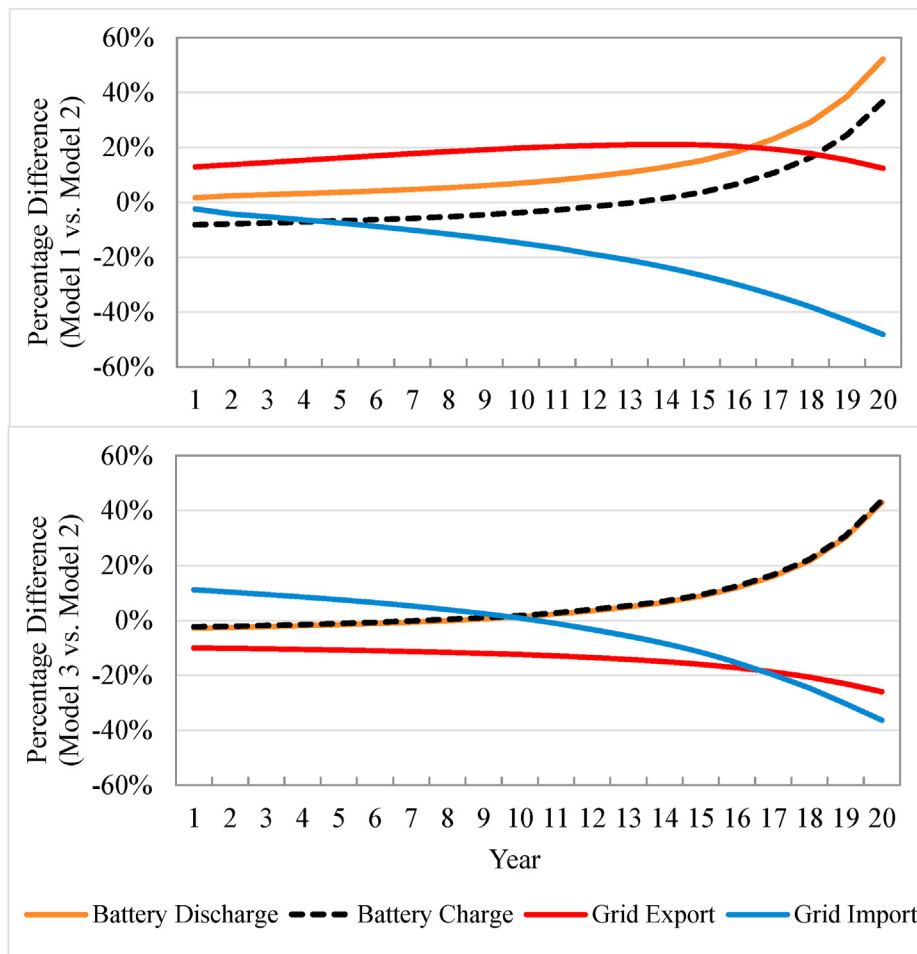


Fig. 8. Impact of model granularity on interactions with the battery and the power grid across the system operating life of 20 years.

Temporal resolution affects simulation results via a couple of aspects: 1) the hour angle calculated at each timestep varies with temporal resolutions and thereby may cause the difference of beam solar irradiance on PV; and 2) the building electrical load varies with the timeframe used to average the 1-s data. The finding on the impact of temporal resolution on simulation results is consistent with the previous work (Beck et al., 2016).

For a given temporal resolution, the impact of model granularity varied significantly with energy flow items and years. The numbers in parentheses in Table 4 represent the percentage differences between the results from Models 1 and 3 and the results from Model 2. These numbers indicated that depending on the number of years that the PV-battery system had operated in the field, Model 1 predicted 3%–15% more PV energy than Model 2 while Model 3 consistently predicted 6% less PV energy than Model 2 for all years. Model 1 over predicted PV energy because it did not consider the impact of temperature and aging on PV module efficiency.

The impact of model granularity on battery charge and discharge as well as on grid export and import cannot be easily inferred from the three years of data in Table 4. Therefore, using Model 2 as the reference, the percentage differences of power flows related to battery and grid interactions are calculated for the other two levels of model granularity over all 20 years. Fig. 8 shows the results. Only results for the cases of 1-min temporal resolution are shown in Fig. 8 because very similar trends have been observed for the other two temporal resolutions. The figure indicates the following:

- The impact of model granularity on battery charge and discharge followed the same trend: the percentage difference increased steadily and slowly for the first 12 years but rapidly for the remaining years. Specifically, relative to Model 2, Model 1 had 2% and 52% more energy for battery discharge respectively in the 1st year and the 20th year, but for battery charge it had 2% less energy in the first year and 37% more energy in the 20th year. In contrast, Model 3 had about 3% less energy for battery charge and discharge than Model 2 in the 1st year but about 43% more energy for battery charge and discharge in the 20th year.

- Model granularity affected grid energy input and export differently. Relative to the intermediate level of model granularity (i.e., Model 2), the coarse granularity (i.e., Model 1) had 12%–21% more energy exported to the grid but up to 48% less energy imported from the grid. In contrast, the refined granularity (i.e., Model 3) had 10%–26% less energy exported to the grid but varied percentage differences of energy imported from the grid, starting from 11% in the 1st year to –36% in the 20th year.

A couple of notes are worth mentioning. First, the percentage differences discussed previously in Table 4 and Fig. 8 may depend heavily on the sizing of PV and battery. In this study, PV and battery are sized large enough to satisfy the instantaneous building loads for most times. The magnitudes of grid energy export and import are small, which may have magnified the corresponding percentage differences. Secondly, all energy flow items are compared in their annual cumulative values. However, close or even identical magnitudes of cumulative energy may have significantly different energy profiles, as will be elaborated in the next subsection.

6.3. Impact of temporal resolution on daily power profiles

To compare the daily power profiles corresponding to the three temporal resolutions, the PV power, battery power and grid power are all generated from Model 2 on the day of March 27. Fig. 9 clearly show the significant difference of all power profiles between the 1-h temporal resolution and the other two temporal resolutions. In particular, though the accumulated daily energy consumption is identical, the load profile with second resolution has many spikes and frequent fluctuations while the hourly profile is much flat.

Spikes of building load and PV power have a large impact on battery charging and discharging. Whether such impact can be accounted for depends on the granularity of battery models. For example, Fig. 10 shows the battery behaviour in the days of March 27–29. All operation variables (i.e., current, voltage and SOC) are generated by the detailed battery model (Model 3). It can be seen from this figure that the battery voltage has been maintained in between the maximum charge voltage and the minimum discharge voltage (i.e., the cut-off voltage). In addition, the

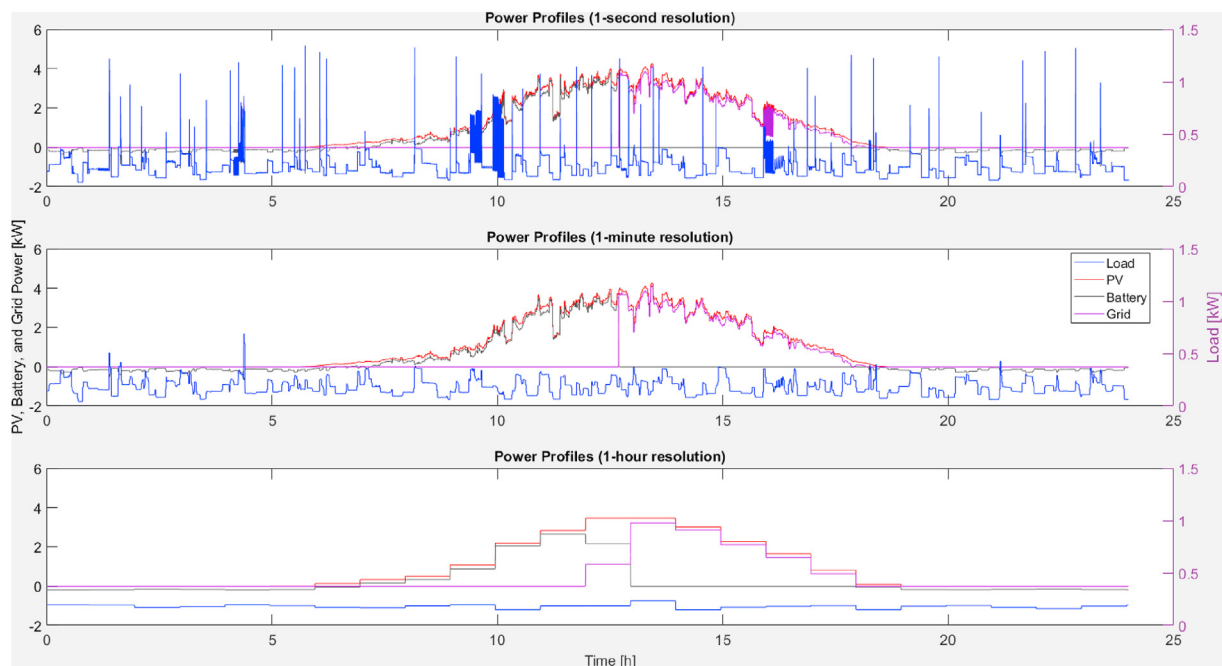


Fig. 9. Comparison of power profiles from the three considered temporal resolutions, namely, 1 s, 1 min, and 1 h. The power for battery charging and grid exportation has positive values while power for battery discharging and grid importation has negative values. The profiles are generated from Model 2.

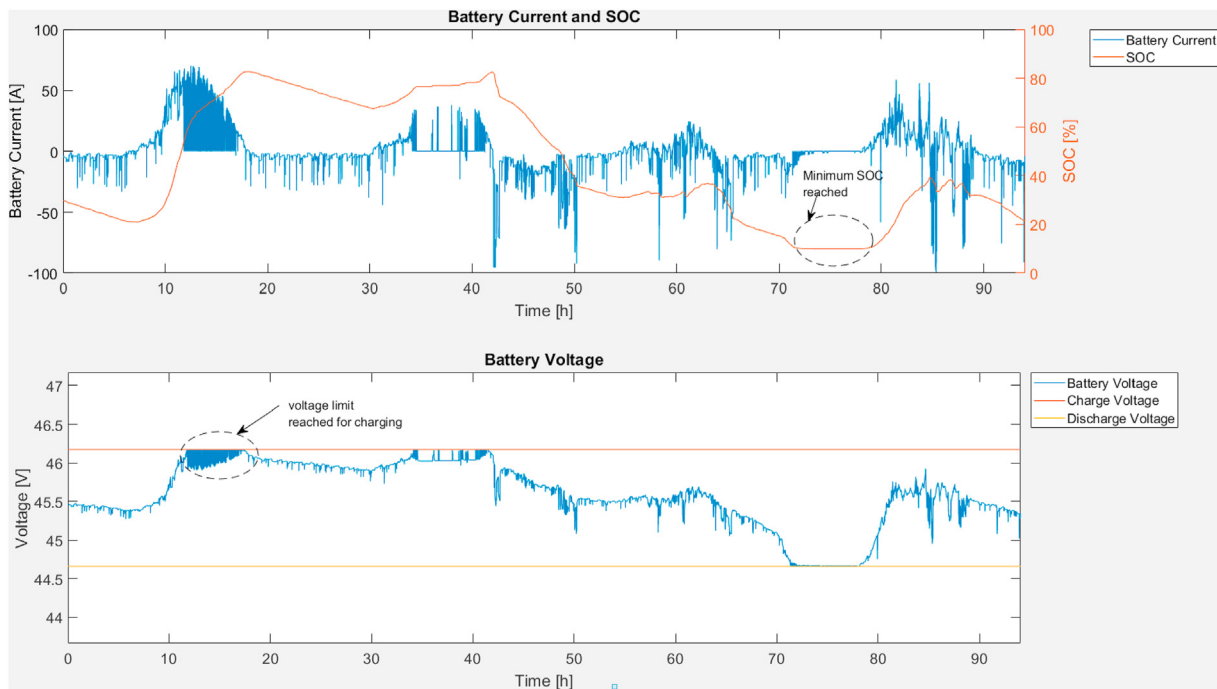


Fig. 10. Example of battery current and voltage limit captured by the detailed battery model. Battery current is positive for charging and negative for discharging.

battery SOC varies within its limits: 10% for the minimum SOC and 90% for the maximum SOC. In this figure, two places are marked where the voltage limit for charging is reached (between the 10th and 20th hour) and the minimum SOC is reached (between the 70th and 80th hour). In both cases, battery is disconnected, as indicated by the battery current being 0 in the upper part of Fig. 10. However, only Model 3 is capable of capturing the limit of charging voltage.

6.4. Comparison of self-consumption and self-sufficiency

Fig. 11 and Fig. 12 respectively show the self-consumption and self-sufficiency of the studied PV battery system at the end of the system lifetime. Similar to the findings on individual energy flow items as discussed in Section 6.1, temporal resolutions had negligible impact on the results. As for the impact of model granularity, the self-consumption was 44% for Model 1, 48% for Model 2, and 52% for Model 3; the self-sufficiency was approximately 83%, 78%, and 80%, respectively for the three models, no matter which temporal resolution was used.

7. Conclusions

PV and battery are the two essential components of residential PV-battery systems. Appropriate models of PV and battery are thus crucial to system performance assessment, optimal design and operational strategy development. For both PV modules and batteries, three models with increasing level of granularity were implemented and compared with respect to their impact on system simulation. The coarse PV model considered the rated electric efficiency only; the intermediate model included the impact of cell temperature and aging on the efficiency of PV power generation; and the refined model used an equivalent electrical circuit model to capture the current-voltage characteristics. Similarly, the coarse battery model regarded the battery as a perfect energy bucket; the intermediate model incorporated the aging impact and the roundtrip efficiency of battery storage; and the refined model used an electrical circuit to capture the battery dynamics under charging and discharging conditions. In addition to model granularity, three temporal resolutions (i.e., 1 s, 1 min, and 1 h) of weather data and building electric loads were considered. A total of 8 simulation scenarios with different combinations

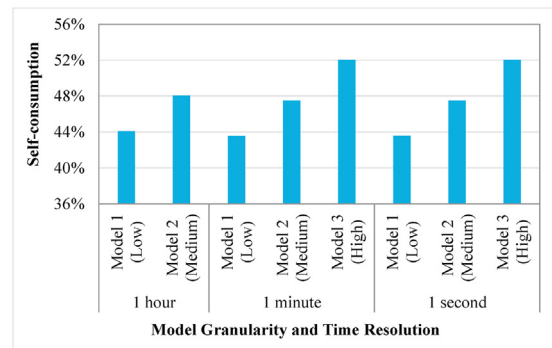


Fig. 11. Self-consumption of the PV-battery system simulated with different model granularity and temporal resolutions. The self-consumption is calculated at the end of the system's 20-year operating life.

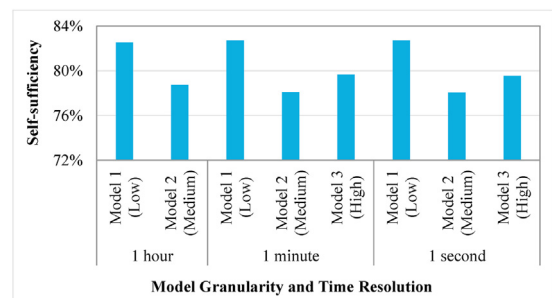


Fig. 12. Self-sufficiency of the PV-battery system simulated with different model granularity and temporal resolutions. The self-sufficiency is calculated at the end of the system's 20-year operating life.

of modelling granularity and temporal resolutions were investigated for a grid-connected residential PV-battery system in Lindenberg, Germany. Major findings from this work include the following:

- For a given modelling granularity, temporal resolutions had a minor impact on the simulated energy flows. All energy flow items had less than 1% difference between the 1-s and 1-min temporal resolutions while up to 10% difference between the 1-h and 1-min temporal resolutions was observed for certain energy flow items. This finding demonstrates that temporal resolution is not critical when cumulative energy flows are the primary consideration (e.g., self-consumption and self-sufficiency).
- Depending on the year of system operation, the coarse PV model (Model 1) predicated 3%–15% more PV energy than the intermediate model (Model 2) while the refined model (Model 3) consistently predicted 6% less PV energy than the intermediate model.
- For all three temporal resolutions, the model granularity had noticeable impact on the power flows that involve the interactions with the battery and the electric grid. The impact of such power profile differences on battery operation can be captured only via the refined battery model.
- When the cumulative energy flows are considered to calculate self-sufficiency and self-consumption, the impact of model granularity can be observed but not much. The self-consumption was approximately 44% for Model 1, 48% for Model 2, and 52% for Model 3; the self-sufficiency was 83%, 78%, and 80%, respectively for the three models.

The work presented in this paper could be extended further in future. First, the impact of model granularity and temporal resolutions could be investigated for other sizing options to understand how the conclusions made from this study could vary with sizing. Secondly, the impact of model granularity on optimal sizing of residential PV-battery systems could be pursued. Given the minor impact of temporal resolutions on power flow items, 1-min resolution of weather and load profiles should be sufficient when pursuing optimization studies.

Declaration of competing interest

We wish to confirm that there are no known conflicts of interest associated with this publication and there has been no significant financial support for this work that could have influenced its outcome.

References

- Anseán, D., Dubarry, M., Devie, A., Liaw, B.Y., García, V.M., Viera, J.C., González, M., 2016. Fast charging technique for high power LiFePO₄ batteries: a mechanistic analysis of aging. *J. Power Sources* 321, 201–209.
- Ardani, K., O'Shaughnessy, E., Fu, R., McClurg, C., Huneycutt, J., Margolis, R., 2016. Installed Cost Benchmarks and Deployment Barriers for Residential Solar Photovoltaics with Energy Storage: Q1 2016 (No. NREL/TP-7A40-67474). National Renewable Energy Laboratory (NREL), Golden, CO.
- Baseline Surface Radiation Network, 2018. World radiation monitoring center. Available at: <https://bsrn.awi.de/data/data-retrieval-via-pangaea/>. (Accessed 18 February 2020).
- Beck, T., Kondziella, H., Huard, G., Bruckner, T., 2016. Assessing the influence of the temporal resolution of electrical load and PV generation profiles on self-consumption and sizing of PV-battery systems. *Appl. Energy*. <https://doi.org/10.1016/j.apenergy.2016.04.050>.
- Brusco, G., Burgio, A., Menniti, D., Pinnarelli, A., Sorrentino, N., 2016. The economic viability of a feed-in tariff scheme that solely rewards self-consumption to promote the use of integrated photovoltaic battery systems. *Appl. Energy*. <https://doi.org/10.1016/j.apenergy.2016.09.004>.
- Burgio, A., Menniti, D., Sorrentino, N., Pinnarelli, A., Leonowicz, Z., 2020. Influence and impact of data averaging and temporal resolution on the assessment of energetic, economic and technical issues of hybrid photovoltaic-battery systems. *Energies* 13 (2), 354.
- Chauhan, A., Saini, R.P., 2014. A review on integrated renewable energy system based power generation for stand-alone applications: configurations, storage options, sizing methodologies and control. *Renew. Sustain. Energy Rev.* <https://doi.org/10.1016/j.rser.2014.05.079>.
- Dubey, S., Sarvaiya, J.N., Seshadri, B., 2013. Temperature dependent photovoltaic (PV) efficiency and its effect on PV production in the world—a review. *Energy Procedia* 33, 311–321.
- Duffie, J.A., Beckman, W.A., 2013. *Solar Engineering of Thermal Processes*. John Wiley & Sons.
- Feldman, D., Margolis, R., 2020. Q2/Q3 2020 Solar Industry Update. U.S. Department of Energy. Available at: <https://www.nrel.gov/docs/fy21osti/78625.pdf>. (Accessed 1 February 2021).
- Hoppmann, J., Volland, J., Schmidt, T.S., Hoffmann, V.H., 2014. The economic viability of battery storage for residential solar photovoltaic systems—A review and a simulation model. *Renew. Sustain. Energy Rev.* <https://doi.org/10.1016/j.rser.2014.07.068>.
- Ibrahim, I.A., Khatib, T., Mohamed, A., 2017. Optimal sizing of a standalone photovoltaic system for remote housing electrification using numerical algorithm and improved system models. *Energy*. <https://doi.org/10.1016/j.energy.2017.03.053>.
- Jordan, D.C., Kurtz, S.R., 2013. Photovoltaic degradation rates—an analytical review. *Prog. Photovoltaics Res. Appl.* 21, 12–29.
- Keil, P., Schuster, S.F., Wilhelm, J., Travi, J., Hauser, A., Karl, R.C., Jossen, A., 2016. Calendar aging of lithium-ion batteries I. Impact of the graphite anode on capacity fade. *J. Electrochem. Soc.* <https://doi.org/10.1149/2.0411609jes>.
- Kosmadakis, I.E., Elmasides, C., Eleftheriou, D., Tsarakakis, K.P., 2019. A techno-economic analysis of a PV-battery system in Greece. *Energies* 12 (7), 1357.
- Langenmayr, U., Wang, W., Jochem, P., 2020. Unit commitment of photovoltaic-battery systems: an advanced approach considering uncertainties from load, electric vehicles, and photovoltaic. *Appl. Energy* 280, 115972.
- Li, J., 2019. Optimal sizing of grid-connected photovoltaic battery systems for residential houses in Australia. *Renew. Energy* 136, 1245–1254.
- Leadbetter, J., Swan, L., 2012. Battery storage system for residential electricity peak demand shaving. *Energy Build.* 55, 685–692.
- Linssen, J., Stenzel, P., Fleer, J., 2017. Techno-economic analysis of photovoltaic battery systems and the influence of different consumer load profiles. *Appl. Energy*. <https://doi.org/10.1016/j.apenergy.2015.11.088>.
- Luna-Rubio, R., Trejo-Perea, M., Vargas-Vázquez, D., Ríos-Moreno, G.J., 2012. Optimal sizing of renewable hybrids energy systems: a review of methodologies. *Sol. Energy*. <https://doi.org/10.1016/j.solener.2011.10.016>.
- Mulder, G., Six, D., Claessens, B., Broes, T., Omar, N., Van Mierlo, J., 2013. The dimensioning of PV-battery systems depending on the incentive and selling price conditions. *Appl. Energy*. <https://doi.org/10.1016/j.apenergy.2013.03.059>.
- Mulleriyawage, U.G.K., Shen, W.X., 2020. Optimally sizing of battery energy storage capacity by operational optimization of residential PV-Battery systems: an Australian household case study. *Renew. Energy* 160, 852–864.
- Nguyen, X.H., Nguyen, M.P., 2015. Mathematical modeling of photovoltaic cell/module/arrays with tags in Matlab/Simulink. *Environmental Systems Research* 4, 24. <https://doi.org/10.1186/s40068-015-0047-9>.
- Okoye, C.O., Solyali, O., 2017. Optimal sizing of stand-alone photovoltaic systems in residential buildings. *Energy*. <https://doi.org/10.1016/j.energy.2017.03.032>.
- Parra, D., Patel, M.K., 2016. Effect of tariffs on the performance and economic benefits of PV-coupled battery systems. *Appl. Energy*. <https://doi.org/10.1016/j.apenergy.2015.11.037>.
- Ried, S., Jochem, P., Fichtner, W., 2015. Profitability of photovoltaic battery systems considering temporal resolution. In: *Proceedings of the 12th International Conference on the European Energy Market (EEM)*.
- Ru, Y., Kleissl, J., Martinez, S., 2013. Storage size determination for grid-connected photovoltaic systems. *IEEE Transactions on Sustainable Energy*. <https://doi.org/10.1109/TSTE.2012.2199339>.
- Sharma, V., Chandel, S.S., 2013. Performance and degradation analysis for long term reliability of solar photovoltaic systems: a review. *Renew. Sustain. Energy Rev.* <https://doi.org/10.1016/j.rser.2013.07.046>.
- Silva, G.D.O., Hendrick, P., 2017. Photovoltaic self-sufficiency of Belgian households using lithium-ion batteries, and its impact on the grid. *Appl. Energy*. <https://doi.org/10.1016/j.apenergy.2017.03.112>.
- SolarWorld, 2018. Sunmodule SW 250 mono. Available at la.solarworld.com/~media/files/pdfs/sunmodule-250-mono-34mm-frame-ds.pdf. (Accessed 18 February 2020).
- Tjaden, T., Bergner, J., Weniger, J., Quaschnig, V., 2015. Representative electrical load profiles of residential buildings in Germany with a temporal resolution of one second. Available at: <https://pvspeicher.htw-berlin.de/veroeffentlichungen/daten/lastprofile/>. (Accessed 2 February 2021).
- Wirth, H., 2018. Recent Facts about Photovoltaics in Germany. Fraunhofer Institute for Solar Energy Systems. Available at: <https://www.ise.fraunhofer.de/content/dam/ise/en/documents/publications/studies/recent-facts-about-photovoltaics-in-germany.pdf>. (Accessed 18 February 2020).
- Yao, L.W., Aziz, J.A., Kong, P.Y., Idris, N.R.N., 2013. Modeling of lithium-ion battery using MATLAB/simulink. In: *Proceedings of the Industrial Electronics Society, IECON 2013-39th Annual Conference of the IEEE*, pp. 1729–1734.
- Zhang, Y., Lundblad, A., Campana, P.E., Benavente, F., Yan, J., 2017. Battery sizing and rule-based operation of grid-connected photovoltaic-battery system: a case study in Sweden. *Energy Convers. Manag.* <https://doi.org/10.1016/j.enconman.2016.11.060>.